International Journal of Applied Earth Observation and Geoinformation 6 (2004) 33–46

INTERNATIONAL JOURNAL OF
APPLIED EARTH OBSERVATION AND GEOINFORMATION

www.elsevier.com/locate/jag

Terra and Aqua: new data for epidemiology and public health

Andrew J. Tatem[a,*], Scott J. Goetz[b], Simon I. Hay[a,c]

[a] *TALA Research Group, Department of Zoology, University of Oxford, South Parks Road, Oxford, OX1 3PS, UK*
[b] *The Woods Hole Research Center, P.O. Box 296, Woods Hole, Massachusetts, MA 02543-0296, USA*
[c] *Kenya Medical Research Institute/Wellcome Trust Collaborative Programme, P.O. Box 43640, 00100 Nairobi GPO, Kenya*

Received 5 December 2003; accepted 5 July 2004

Abstract

Earth-observing satellites have only recently been exploited for the measurement of environmental variables of relevance to epidemiology and public health. Such work has relied on sensors with spatial, spectral and geometric constraints that have allowed large-area questions associated with the epidemiology of vector-borne diseases to be addressed. Moving from pretty maps to pragmatic control tools requires a suite of satellite-derived environmental data of higher fidelity, spatial resolution, spectral depth and at similar temporal resolutions to existing meteorological satellites. Information derived from sensors onboard the next generation of moderate-resolution Earth-observing sensors may provide the key. The MODIS and ASTER sensors onboard the Terra and Aqua platforms provide substantial improvements in spatial resolution, number of spectral channels, choices of bandwidths, radiometric calibration and a much-enhanced set of pre-processed and freely available products. These sensors provide an important advance in moderate-resolution remote sensing and the data available to those concerned with improving public health.

Keywords: Remote sensing; Terra; Aqua; MODIS; ASTER; Vector-borne diseases

1. Introduction

For the past 30 years, the sensors on Earth-observing satellites have provided an unprecedented view of the land surface, but have only more recently been exploited for the measurement of environmental variables of relevance to epidemiology and public health (Hay, 1997, 2000; Hay et al., 1997; Kazmi and Usery, 2000; Thomson and Connor, 2000). A wide-variety of vector-borne diseases have been investigated (Randolph, 2000; Rogers et al., 2002a; Tatem et al., 2003) but predominant among the interests of the authors have been the application of remotely sensed data to describing spatial distribution and temporal dynamics of malaria epidemiology in sub-Saharan Africa (Hay et al., 2000a; Omumbo et al., 2002). There are between 300 and 500 million clinical cases of the mosquito-borne disease malaria every year,

* Corresponding author. Tel.: +44 1865 271262; fax: +44 1865 310447.
E-mail address: andy.tatem@zoo.ox.ac.uk (A.J. Tatem).

0303-2434/$ – see front matter
doi:10.1016/j.jag.2004.07.001

resulting in 1–3 million deaths, of which over 90% occur in sub-Saharan Africa (Greenwood and Mutabingwa, 2002; Sachs and Malaney, 2002). Every 40 s a child dies of malaria, rendering it one of the top global killers and a massive barrier to development in Africa. Sadly, despite years of progress fighting the disease, drug and insecticide resistance, underfunding, along with environmental, climatic and population changes, have meant that mortality from malaria is now increasing once again in sub-Saharan Africa.

Empirical malariometric data in combination with environmental information from Earth-observing satellites have now been used to map mosquito vector distributions, the force of infection as measured by annual entomological inoculation rates, disease prevalence using parasite rate surveys and malaria seasonality (for a review, see Hay et al., 1998; Rogers et al., 2002b). The justifications for such maps (Snow et al., 1996) include (a) informing the appropriate choice of malaria control, since different control options are optimal in different endemic settings; (b) an evidence-base to planning the magnitude of control operations by determining population at risk; (c) defining optimal and equitable spatial targeting of interventions; (d) determining optimal timing of control, for example, when in the year to impregnate bed-nets with insecticide and (e) assisting in the assessment of control interventions by documenting reduction in malaria with respect to pre-intervention levels. These efforts have been achieved at continental and regional scales and at higher spatial resolutions for specific sub-regional and county level areas of interest.

While this initial round of work has been valuable in establishing methodological approaches and a macro-level understanding of malaria distribution and burden, it has become more obvious that to fully utilize such information for an increased evidence-base for malaria planning and control, several limitations need to be addressed. Among these are the need to define more accurately human population distribution and the effects urbanization, water body distribution and land use have on these often spatially-coarse malaria transmission, prevalence and morbidity estimates. The higher spatial resolution of disease information needs to be combined in decision-support systems that require much more detailed information on health facility and service delivery infrastructure than is currently available. The high temporal, spatial and spectral resolution of sensors onboard NASAs Terra and Aqua satellites offer a significant opportunity in providing the data to help address some of these limitations. It is these data and their potential utility for future public health studies that are the focus of the current review. Not only does this review aim to distil salient information from a diverse and usually unfamiliar literature to those concerned with both public health and remote sensing, but also to highlight the important considerations with reference to use of these data in epidemiological and public health applications.

2. Earth-observing systems EOS AM-1 and EOS PM-1: Terra and Aqua

Launched in December 1999 and May 2002 respectively, Terra (or EOS AM-1) and Aqua (or EOS PM-1) are the first of a series of multi-instrument spacecraft forming NASAs Earth Observing System (EOS). EOS consists of a science component and a data information system (EOSDIS) supporting global observations of the land surface, biosphere, solid Earth, atmosphere and oceans (USGS/NASA, 2002a). EOS is scheduled to provide at least an 18-year data set, allowing short-term anomalies, natural interannual to interdecadal oscillations, as well as human induced changes to be distinguished (Kaufman et al., 1998). To meet these measurement objectives, EOS data is being collected over a wide spectral range and both high and moderate spatial resolutions with a variety of observation strategies. The primary mission of Terra is to ‘‘perform high accuracy measurements of the main parameters that describe the state of the Earth and its atmosphere, and begin a long-term monitoring of the human impact on the environment’’ (Kaufman et al., 1998). In contrast, Aqua’s mission has a particular emphasis ‘‘on water as it exists throughout the atmosphere, both on or near the Earth’s surface, including water in its liquid, solid and vapour forms’’ (Parkinson et al., 2003). Although such broad aims are primarily focussed on quantifying and monitoring environmental change, the same data have considerable potential in public health application.

Both Terra and Aqua travel in sun-synchronous, near-polar orbits with 10.30 and 1.30 a.m./p.m. equatorial crossing times respectively to minimise cloud effects of observations of the Earth's surface, since such effects lower reflectance values, and introduce error into the picture obtained of the Earth below. Terra has five complementary scientific instruments, and Aqua has six, each calibrated to a higher degree than any comparable sensor (Kaufman et al., 1998). These instruments will attempt to extend measurements of their ''heritage'' sensors (e.g. Advanced Very High Resolution Radiometer (AVHRR) and the Coastal Zone Color Scanner (CZCS)), but with a higher degree of precision in addition to taking new measurements.

This review focuses principally on the two instruments that have the most obvious public health and epidemiological applications: MODIS and ASTER. The other sensors onboard Terra and Aqua are designed primarily for atmospheric studies and their potential benefits are only briefly outlined at the end of this review.

3. The moderate-resolution imaging spectroradiometer (MODIS)

The MODIS is a key instrument onboard Terra and is complemented by another MODIS on the Aqua satellite. The MODIS sensors display substantial improvements in spatial resolution, number of spectral channels, choices of bandwidths, radiometric calibration and a much-enhanced set of derived products over that of the AVHRR sensors (Townshend and Justice, 2002) that formed the basis of broad spatial-scale epidemiological studies (Hay, 1997, 2000). Table 1 details these specifications. Although other moderate spatial resolution sensors have been launched into orbit in recent years, factors such as charging policies, mission lifespan and an oceanographic focus, make them far less attractive to the public health community. Particularly relevant to the design of the land-imaging component is the incorporation of characteristics of the AVHRR sensor to provide continuity in temporal image sequences with existing global archives (Justice et al., 1998).

Temporal, spatial and spectral resolutions are all extremely important factors in determining the utility of a satellite-based sensor for epidemiological and public health studies. The low frequency of image capture for any point on the Earth for high spatial resolution sensors such as Landsat Thematic Mapper (TM, 16 days), means that few cloud-free images can be obtained, especially over the equatorial tropics, limiting the possibilities of building complete temporal records of environmental variables. In turn, this has limited the use of such sensors in epidemiology and public health, and favoured moderate/coarse-resolution sensors such as the AVHRR with repeat times as small as 12 h (Hay, 2000). The MODIS on the Terra and Aqua platforms has an image capture time of 1–2 days (effectively improves to 12–24 h when utilising both sensors), but MODIS also provides significant increases in spatial and spectral resolution over the AVHRR. With 36 spectral bands and 12-bit radiometric resolution, MODIS has the highest number of spectral bands of any global-coverage moderate-resolution imager (Justice et al., 2002). Table 2 details these bands and their primary uses. The larger number of bands allows more accurate meteorological and other ecological variables to be derived. Moreover, the channels have smaller waveband ranges than any other moderate-resolution images, allowing exploitation of 'spectral windows' where atmospheric signal attenuation is minimal.

3.1. Temporal continuity with existing archives

Continuity with existing imagery archives is vital if attempts to link climate variables with temporal disease cycles and dynamics are to be comprehensively

Table 1
Characteristics of the moderate-resolution imagine spectroradiometer (MODIS)

Orbit	705 km altitude, sun-synchronous orbit, near-polar nominal descending equatorial crossing at 10.30 a.m. local time
Swath	2330 km $\pm$ 55° cross-track
Spectral bands	36 bands, between 0.405 and 14.385 μm
Radiometric resolution	12 bits
Spatial resolutions (at nadir)	250 m (bands 1–2), 500 m (bands 3–7), 1000 m (bands 8–36)
Repeat coverage	Daily, north of 30° latitude, every 2 days for <30° latitude

Table 2
Spectral bandpass details of the moderate-resolution imaging spectroradiometer (MODIS)

Primary use	Band number	Spectral range (μm)	Spatial resolution (m)
Land/cloud/aerosols/boundaries	1	0.62–0.67	250
	2	0.841–0.876	
Land/cloud/aerosols/properties	3	0.459–0.479	500
	4	0.545–0.565	
	5	1.230–1.250	
	6	1.628–1.652	
	7	2.105–2.155	
Ocean colour/phytoplankton/biogeochemistry	8	0.405–0.420	1000
	9	0.438–0.448	
	10	0.483–0.493	
	11	0.526–0.536	
	12	0.546–0.556	
	13	0.662–0.672	
	14	0.673–0.683	
	15	0.743–0.753	
	16	0.862–0.877	
Atmospheric water vapour	17	0.890–0.920	1000
	18	0.931–0.941	
	19	0.915–0.965	
Surface/cloud temperature	20	3.660–3.840	1000
	21	3.929–3.989	
	22	3.929–3.989	
	23	4.020–4.080	
Atmospheric temperature	24	4.433–4.498	1000
	25	4.482–4.549	
Cirrus clouds water vapour	26	1.360–1.390	1000
	27	6.535–6.895	
	28	7.175–7.475	
Cloud properties	29	8.400–8.700	1000
Ozone	30	9.580–9.880	1000
Surface/cloud temperature	31	10.780–11.280	1000
	32	11.770–12.270	
Cloud top altitude	33	13.185–13.485	1000
	34	13.485–13.785	
	35	13.785–14.085	
	36	14.085–14.385	

studied. The inclusion of spectral bands similar to those of Landsat TM and AVHRR within the 36 bands of MODIS will facilitate this, although clearly the finer spectral resolution of MODIS will provide different information than the broader bandwidths of the AVHRR. For example, radiation absorption by atmospheric constituents, particularly ozone and water vapour, have been well documented in the AVHRR record – and have led to development of approaches to estimate these important variables for information on the atmosphere rather than the land surface. Numerous other issues arise when attempting to provide continuity between the AVHRR record and the MODIS observational period. The long-term record from the early 1980s for terrestrial vegetation observations has been derived from afternoon-overpass AVHRR data, hence the 10.30 a.m. overpass of Terra's MODIS will provide surface reflectance information that differs due to diurnal variation in sensor-solar illumination geometry (Townshend and Justice, 2002), as well as potentially dramatic differences in thermal observations and associated land surface temperature (LST) estimates (Gutman, 1999; Gleason et al., 2002). Whereas many of the nuances of AVHRR observational data have been at least partly addressed, including substantial drift in the orbital crossing time at any given location, there are several additional factors that influence data set continuity. One of these is introduced by the improved radiometric and spatial resolution of MODIS sensors. Spatial scaling of MODIS to AVHRR resolution is easily accomplished through data resampling techniques but cannot, for example, account for the unique sampling strategy used in the production of the AVHRR 64 km^2 global area coverage (GAC) data sets from the nominal 1.2 km^2 local area coverage (LAC) (Justice et al., 1995). Moreover, spatial scaling of radiometric observations even to LAC resolution may be nonlinear, which introduces the need for more sophisticated scaling strategies than simple regression (Hall et al., 1992; Dubayah et al., 1997). The Earth science community and funding agencies have recognized the importance of continuity in the satellite observational data sets. Several efforts have been initiated to ensure the valuable 20+ year AVHRR time series can be continued, and improved upon, with MODIS and other follow-on missions (e.g., National Polar-orbiting Operational Environmental Satellite System (NPOESS), Visible and Infrared Imaging Radiometer Suite (VIIRS) (NPOESS, 2003)).

In addition to MODIS bands 1 and 2, acquiring global data at an unprecedented 250 m resolution, detailed continuous monitoring of other environmental variables relevant to epidemiology and public health can potentially also be produced using the 500 m and 1000 m spatial resolutions of bands 3–36. Fig. 1(a) and (b) demonstrate the improvement in spatial resolution of the MODIS (500 m spatial resolution) over the AVHRR (1.1 km spatial resolution) for Kisumu, Kenya, an area of significant epidemiological interest. Such a spatial resolution improvement potentially facilitates significant advances in the temporal analysis and mapping of vector distributions, infection rates and disease prevalence of both malaria and other vector-borne diseases across the globe. Fig. 1 clearly shows that the detail now obtainable from the MODIS imagery represents an advance in the utility of the imagery to identify more local-scale features overlooked when conducting studies based on AVHRR imagery. The environmental and climatic variables obtainable from MODIS will be described and discussed in the following paragraphs.

3.2. MODIS environmental and climatic variables

Throughout the brief history of remotely sensed imagery use within epidemiology and public health, the time-consuming process of atmospherically correcting, geo-registering, compositing and processing satellite imagery to produce accurate environmental variables has always been a constraint, not least because most epidemiologists are unfamiliar with such processes. In addition, the number of different algorithms used to produce variables such as land surface temperature has lead to incomparable results (Kalluri and Dubayah, 1995). This is true of many other fields of environmental research and the MODIS imagery production team have recognised this, and now standard higher-order data products are being continuously produced and archived (Justice et al., 2002). In fact, products from the MODIS include the most comprehensive quality assessment metadata ever produced in the context of terrestrial and atmospheric remote sensing (Roy et al., 2002). This enables the resources of other scientists to be focussed on answering the relevant scientific questions, rather than optimizing data processing. This is particularly important due to the high data volumes associated with MODIS. Satellite-derived vegetation indices, LST, middle infrared radiation (MIR) and land cover estimates have all been shown to be related to facets of vector-borne diseases, and thus used to some degree in epidemiological studies in the past (Hay, 2000). The advanced specifications of MODIS means that these variables can now be produced at finer spatial resolutions than before and, through the MODIS processing procedure, are available atmospherically corrected, geo-registered, composited and at no cost to the user.

In addition to satellite-derived climate variables, many recent epidemiological studies have made use of the link between vegetation amount and vector populations via the application of normalized difference vegetation index (NDVI) imagery. MODIS products now allow the epidemiological research

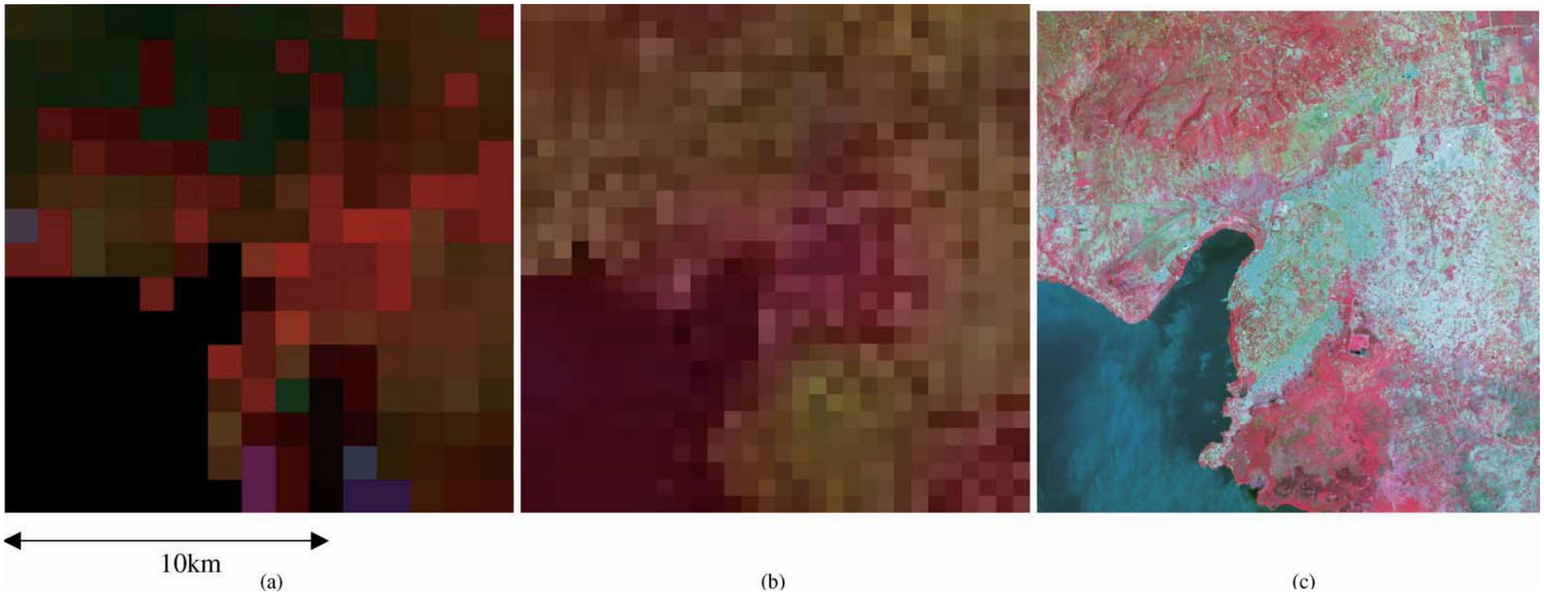

Fig. 1. (a) NOAA AVHRR image of Kisumu, Kenya (1.1 km spatial resolution), historically the principal imagery type used in epidemiological studies; (b) Terra MODIS image of Kisumu, Kenya (500 m spatial resolution) demonstrating the improvement in spatial resolution over AVHRR, potentially facilitating more accurate mapping of vector distribution, disease prevalence and infection rates; (c) Terra ASTER image of Kisumu, Kenya (15 m spatial resolution) where areas of settlement are clearly visible, enabling the examination of populations at risk, leading to improved disease burden estimates.

community to move beyond its previous dependence on the NDVI, which has always represented a key part of vector-borne disease studies (Hay, 2000). A new MODIS product, the enhanced vegetation index (EVI), offers improvements over the NDVI, reducing saturation of the signal at high vegetation coverages and reducing soil background effects (Heute et al., 2002). Should continuity with previous studies need to be maintained, the NDVI is also available, and imagery of both indices can be obtained at 250 m or 1 km spatial resolution, and as 16-day or monthly images. Fig. 2(a) shows an example of 250 m spatial resolution NDVI imagery for western Europe, an area increasingly being threatened by unprecedented incursions of vector-borne diseases previously confined to Africa and Asia (Gratz, 1999; Randolph, 2001; Tatem et al., 2003). As noted, even at comparable spatial resolution, standard NDVI values derived from MODIS and historical AVHRR would not be entirely comparable, due to the improved spectral and radiometric properties of the MODIS sensors and differences in acquisition time. Applications of both MODIS and AVHRR data have, however, developed methods to compensate for these differences (e.g. Hansen et al., 2002), much of which can be overcome by statistical regression using coincident data sets over a common location.

As well as NDVI, satellite-derived LST estimates have commonly proved central to recent epidemiological studies (e.g. (Rogers et al., 2002a,b)). LST estimates at day-or-night are available with daily, 8-day or monthly temporal frequency, and at 1 or 5 km spatial resolutions from processed MODIS imagery. Previous derivations of LST estimates within epidemiology have more often than not relied on 'split-window' approaches using a simple combination of AVHRR bands 4 and 5 (Price, 1984; Kalluri and Dubayah, 1995; Hay and Lennon, 1999; Goetz et al., 2000; Hay et al., 2000b; Green and Hay, 2002). The accuracy of these results is, however, limited by the knowledge of the spectral emissivity and its angular variations (Justice et al., 1998; Schmugge et al., 2002). MODIS LST product production uses two more complex approaches, which have been shown to produce LST with an accuracy of ± 1 K (Petitcolin and Vermote, 2002). An example of the MODIS LST product is shown for western Europe in Fig. 2(b). LST is derived using either a split-window method that takes into account land surface emissivity (Snyder et al., 1998) or a "full up" atmospheric correction method that requires knowledge of atmospheric properties both spatially and temporally (Wan and Li, 1997). Comparability of these LST estimates with those derived from AVHRR imagery and, consequently, the validity of long-term time series analysis, remains an important consideration of epidemiological applications. The primary issue with thermal data continuity in MODIS and AVHRR is the image acquisition time. Methods to correct AVHRR observational time series data for acquisition time have been developed using both statistical (Gutman, 1999; Gleason et al., 2002) and thermal modelling approaches (Jin and Dickeson, 1999), but have not yet been developed for MODIS data continuity purposes. Until advances in cross-comparability are more widely available, an interim solution may be to derive LST from MODIS and AVHRR using the same approach, and then develop per-pixel correction techniques based on statistical regression analyses for a common area.

Aside from the vegetation indices and LST estimates commonly used in recent epidemiology and public health studies, other useful variables are available as MODIS products. Middle infrared has been shown to be correlated with the surface temperature, water content and structure of vegetation canopies, and suffers little attenuation by the atmosphere (Boyd and Curran, 1998). MIR spectral bands are available as a MODIS product at 250 m, 500 m or 1 km spatial resolutions, with temporal frequencies of daily or 8 days. An example of MODIS MIR imagery at 500 m spatial resolution is shown in Fig. 2(c) for western Europe. Land cover may be important in epidemiology, but consistency between land cover maps has, in the past, been difficult to obtain due to the vast array of imagery, classifiers, class descriptions and validation approaches (Curran et al., 2000). In producing MODIS land cover and land cover change products at 250 m, 500 m, 1 km and 25° spatial resolutions every 3 months, some standardisation must be implemented (Justice et al., 1998).

A large number of other MODIS products exist, which have previously not been used in epidemiology and public health, but may have future potential. These include albedo, land surface bi-directional distribution functions, leaf area indices, fire distribution, snow and

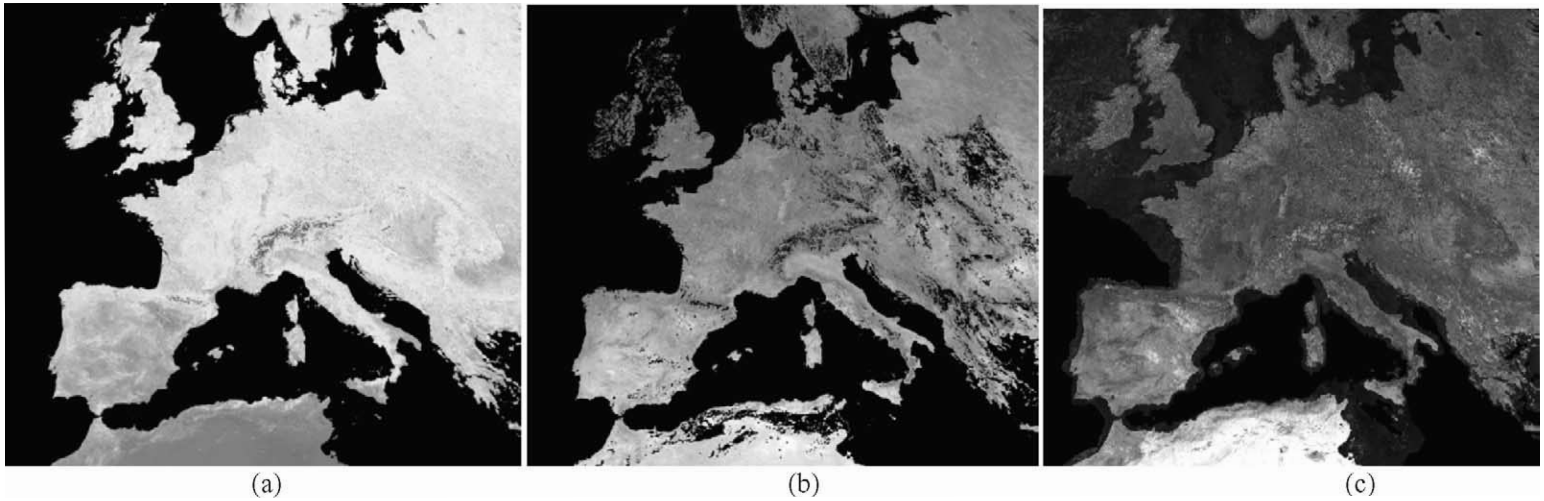

Fig. 2. MODIS standard data products of proven epidemiological significance for western Europe: (a) normalised difference vegetation index (250 m spatial resolution); (b) land surface temperature (1 km spatial resolution); (c) middle infrared reflectance (500 m spatial resolution). These improvements in spatial resolution over the well-used AVHRR imagery, combined with disease and vector data provide opportunities for more accurate disease risk and vector distribution estimates.

ice cover, various oceanographic products and surface reflectances from all the 36 spectral bands.

The provision of just spectral reflectance information meant that, throughout the history of the AVHRR, much work was undertaken on the derivation of climatic and environmental variables, with the fields of epidemiology and public health benefiting from this. The provision of 36 reflectance bands from MODIS means that an even greater potential exists to produce further data products than those produced centrally by NASA. Certain environmental and climatic variables, not described already, have often proved to be of great relevance to epidemiological and public health research problems. Examples of these include air temperature, humidity, vapour pressure deficit, surface wetness and soil moisture, all of which have been derived in the past from AVHRR imagery (Goetz et al., 2000; Hay, 2000). Similar approaches can be applied to MODIS imagery to derive useful environmental indicators, and substantial progress has already been made by the Terra and Aqua facility instrument teams (NASA, 2003).

4. The Advanced Spaceborne Thermal Emission and Reflection Radiometer (ASTER)

While MODIS represents a key instrument in advancing the study of vector-borne diseases at continental to global scales, the ASTER is a valuable tool in studying and understanding processes at local to regional scales. As the only high spatial resolution instrument onboard Terra or Aqua, ASTER provides the 'zoom lens' for the other instruments. Such a utility enables the epidemiologist to focus on smaller-scale studies in areas of interest identified in large-scale studies by AVHRR or MODIS imagery. Local-scale public health studies utilizing satellite imagery have traditionally relied upon Landsat Thematic Mapper (TM) or SPOT High Resolution Visible (HRV) imagery to carry out basic mapping (Dister et al., 1997; Hay, 1997; Hay et al., 1998). In a similar manner to the way MODIS displays substantial improvements over its predecessor, AVHRR, so ASTER represents the next step on from the SPOT HRV and Landsat TM. Fig. 1(c) demonstrates the detail obtainable using the fine spatial resolution of ASTER imagery for Kisumu, Kenya, compared to that of AVHRR (Fig. 1(a)) and MODIS (Fig. 1(b)). Fig. 1(c) demonstrates the potential of the imagery in clearly defining settlement extent and type, enabling more accurate estimates of populations at risk and disease burden. The ASTER sensors display improvements in spatial resolution, number of spectral channels, radiometric calibration, choice of bandwidths, range of derived products and, most importantly in many cases, the cost of imagery compared to their counterparts. Although many high spatial resolution sensors have been launched in recent years, factors including spectral band limitations, mission lifespans and charging policies, make them less attractive to the field of public health and epidemiology than ASTER. This is particularly true when one considers that those areas of the world where vector-borne diseases pose the greatest obstacles are those where funds for control and research are the least.

ASTER is a cooperative effort between NASA and Japan's Ministry of Economic Trade and Industry (METI) with the collaboration of scientific and industry organisations in both countries (Kahle et al., 1991). The sensor covers a wide spectral region with 14 bands from the visible to the thermal infrared (TIR), with high spatial, spectral and radiometric resolution. Table 3 details ASTERs bandpass specifications and shows how spatial resolution varies with wavelength: 15 m in

Table 3
Spectral bandpass details of the Advanced Spaceborne Thermal Emission and Reflection Radiometer (ASTER)

Subsystem	Band number	Spectral range (μm)	Spatial resolution (m)
VNIR	1	0.52–0.60	15
	2	0.63–0.69	
	3N	0.78–0.86	
	3B	0.78–0.86	
SWIR	4	1.600–1.700	30
	5	2.145–2.185	
	6	2.185–2.225	
	7	2.235–2.285	
	8	2.295–2.365	
	9	2.360–2.430	
TIR	10	8.125–8.475	90
	11	8.475–8.825	
	12	8.925–9.275	
	13	10.25–10.95	
	14	10.95–11.65	

Taken from Yamaguchi et al. (1998).

visible and near infrared (VNIR), 30 m in the shortwave infrared (SWIR) and 90 m in the thermal infrared. ASTER can acquire around 650 scenes per day, each covering an area 60 km × 60 km. The three VNIR bands were designed to have similar bandpasses to those of the Landsat TM and the optical sensor (OPS) of the Japanese Earth Resources Satellite (JERS-1) (Yamaguchi et al., 1998). This design should allow for possible comparisons between previous epidemiological studies made using these sensors and new studies using ASTER. It also allows for potential consistent temporal monitoring of specific areas to continue, despite the introduction of a new generation sensor. Such a feature is vital if long-term studies of disease cycles or changes in populations at risk are to be undertaken. As described for MODIS however, inconsistencies between ASTER and its predecessor sensors mean great care must be taken to ensure confident comparisons can be made. The spectral ranges of the SWIR bands were selected mainly for the purpose of surface soil and mineral mapping (Yamaguchi et al., 2001), but reflectance measurements in the 2–4 μm range (also known as MIR) are correlated with surface temperature, water content and structure of vegetation canopies, and therefore, of use in epidemiological studies. Finally, the multispectral TIR data allows for a more accurate determination of the variable spectral emissivity of the land surface and a more accurate determination of the LST (Fujisada, 1994).

As with MODIS imagery, a large part of the time-consuming process of atmospheric correction, geo-registration, composition and processing of ASTER imagery has been reduced by the provision of readily available ASTER products. Whereas a vast array of higher-order products are produced and archived from MODIS imagery, many with obvious public health applications, the range available from ASTER imagery is not as comprehensive. Satellite-derived LST has a history of use within epidemiology and public health, and the advent of ASTER means that this information is now available at 90 m spatial resolution at low cost (Gillespie et al., 1998). The provision of LST imagery as a higher-order product should also introduce consistency in LST derivation, leading to more direct cross-comparability between different local-scale studies.

Due to the topographically restricted distributions of many vectors of disease, a commonly-used product in epidemiology and public health studies is the digital elevation model (DEM), and most of the studies that have incorporated a DEM have used the 1 km spatial resolution USGS model (USGS/NASA, 2002b). The VNIR backward viewing band of ASTER now allows for high spatial resolution stereoscopic observation and the consequent production of a DEM product. With a 30 m spatial resolution, 7 m height accuracy and coincident registration with other ASTER imagery, the DEM product represents a potentially valuable source of altitude information for small-scale epidemiological studies. Compared to the ready-for-use wide product range of MODIS, the provision for ASTER of just LST and a DEM may seem disappointing from a public health and epidemiology perspective. However, surface reflectance imagery is available from which further relevant environmental and climatic variables can be derived. These may include NDVI at 15 m spatial resolution from the VNIR bands, use of the middle infrared bands as they are, derivation of air temperature estimates from LST and NDVI at 90 m spatial resolution, and land cover or ecozones through supervised or unsupervised classification of all bands. The challenge exists to continue the epidemiological work undertaken with AVHRR imagery (Anyamba and Eastman, 1996; Linthicum et al., 1999; Goetz et al., 2000; Hay, 2000) in producing new environmental and climatic variables from ASTER imagery.

5. Other instruments onboard Terra and Aqua

Aside from MODIS and ASTER, Terra carries three other instruments and Aqua carries five others, all of which have less obvious application within the field of epidemiology and public health, but in a desire to be comprehensive, references are provided here. Nevertheless, the novel, unique and high quality data that each produces has great potential to be used to create climate and environmental variable imagery of potential epidemiological and public health application, in addition to providing parameters for improving and calibrating MODIS and ASTER-derived variables.

5.1. CERES

Both Terra and Aqua carry two Clouds and Earth's Radiant Energy System (CERES) instruments. These radiation scanners provide measurements of cloud amount, height, optical depth, particle size and phase for use in global climate models (Wielicki et al., 1998). The design of the instrument attempts to build upon work undertaken by previous missions, such as the Earth radiation budget experiment (ERBE) (Barkstrom, 1984), by providing a better understanding of the role of clouds and the energy cycle in global climate change. While such an aim may not appear coincident with those of the epidemiology and public health research community, potential exists to utilise this rich source of climate data. The design of CERES enables the possible derivation of daily rainfall, land cover change and natural hazard information at 20 km spatial resolution. Such a data series, especially if linked up to archive ERBE data, could provide a valuable tool in the study of disease temporal dynamics.

5.2. MISR

The multi-angle imaging spectro-radiometer (MISR) aims to study how sunlight is scattered to determine how changes in amounts, types and distribution of clouds, airborne particles and surface cover affect our climate. This is achieved by imaging the Earth in nine different view directions to infer the angular variation of reflected sunlight, and the physical characteristics of observed scenes (Diner et al., 1998). In addition to the main aim of improving understanding of the fate of sunlight in Earth's environment, MISR data can also distinguish different types of clouds, particles and surfaces. Specifically, MISR monitors the monthly, seasonal and long-term trends in (a) the amount and type of atmospheric particules, (b) the amounts, types and heights of clouds, (c) the distribution of land surface cover, including vegetation canopy structure (Diner et al., 2002). As with CERES, MISR data represents an untapped resource for the epidemiology and public health community, of both climate and land cover data, at a standard not seen before. MISRs design is novel and unique, causing researchers around the world to experiment and determine its potential benefits in a wide range of fields, and there is no reason to believe that epidemiology and public health should not also reap the benefits of such a tool.

5.3. MOPITT

The measurements of pollution in the troposphere (MOPITT) instrument provides global CO maps in three altitude layers and global CH_4 maps with 22 km spatial resolution (Drummond and Mand, 1996; Deeter et al., 2002). This is perhaps the instrument onboard Terra with the least obvious public health and epidemiological application, due to these very specific aims. However, this does not mean its data should be overlooked, as potential exists to utilise the imagery produced to provide climate information of relevance to public health and epidemiology. An example of such alternative applications was given by Warner et al. (2001), whereby MOPITT imagery was used for cloud detection and cloud-top height retrieval, leading to a possible surface radiation monitoring approach.

5.4. AIRS

The atmospheric infrared sounder (AIRS) is a 2382-channel high spectral resolution sounder, focussed primarily on the infrared portion of the spectrum (Aumann et al., 2003). Its main purpose is to obtain atmospheric temperature and humidity profiles at a spatial resolution of 13.5 km from the land surface upward to an altitude of 40 km (Parkinson, 2003). While this appears to offer valuable information on climate variables central to epidemiological studies, simulations suggest that no more than 5% of the AIRS field of view will be cloud-free (Parkinson, 2003), reducing its utility to such research.

5.5. AMSU

The advanced microwave sounding unit (AMSU) is a 15-channel sounder designed to work in tandem with AIRS to reduce the effects of clouds (Susskind et al., 2003). Its aim is again to produce atmospheric temperature profiles but, at a spatial resolution of 40.5 km, the imagery is only likely to match the scales required by global public health studies.

5.6. HSB

The humidity sounder for Brazil (HSB) forms the third part of Aqua's integrated cross-track scanning temperature and humidity sounding system with AIRS and AMSU. While it does only have four channels, the positioning of these in water absorption bands, make HSB a potentially useful tool for epidemiology and public health. The HSB provides measurements at 13.5 km spatial resolution of humidity, cloud liquid water, precipitation and precipitable water (Lambrigtsen and Calheiros, 2003), all variables of relevance to disease vector populations. Unlike AIRS, however, its use of microwave channels means the data is unaffected by cloud cover, and therefore of greater application in epidemiology and public health studies requiring near-surface variables.

5.7. AMSR-E

The advanced microwave scanning radiometer for EOS (AMSR-E) is a 12-channel conically scanning passive-microwave radiometer measuring vertical and horizontal polarized radiation (Kawanishi et al., 2003). Provided by the National Space Development Agency of Japan (NASDA), it builds on the heritage of previous passive-microwave instruments, providing improved spatial resolution of 5–56 km depending on the channel. AMSR-E data will form the basis of a vast range of data products, including measurements of rainfall, water vapour, cloud water, wind speed, snow depth and soil moisture (Njoku et al., 2003), making it potentially very attractive to the epidemiology community for derivation of vector-affecting variables unobtainable through MODIS due to cloud cover. The all-weather day-or-night capability of AMSR-E in obtaining surface variables complements the fine spatial resolution of MODIS, potentially enhancing the value of the Aqua mission to those in public health.

6. Conclusions

Both Terra and Aqua represent important advances in remote sensing at local to continental scales, and the data for epidemiology and public health studies are exceptional, providing new spatial and spectral data with exciting possibilities for the field as a whole. The epidemiology and public health community has been relatively slow to adopt new products derived from remote sensing. Our aim here has not been to define research objectives, but to provide an overview of the advances facilitated by these valuable observational data sets, as well as some of the realistic considerations for their use in epidemiological applications at a range of spatial and temporal scales. In an era of public health where donor support for the upscaling of research into regional interventions is increasing, techniques that can help map and monitor changes in the environment relevant to epidemiology will be increasingly called upon for modelling and evaluating impacts.

References

Anyamba, A., Eastman, J.R., 1996. Interannual variability of NDVI over Africa and its relationship to El Niño/Southern Oscilliation. Intl. J. Remote Sensing 17, 2533–2548.

Aumann, H.H., Chahine, M.T., Gautier, C., Goldberg, M.D., Kalnay, E., McMillin, L.M., Revercomb, H., Rosenkranz, P.W., Smith, W.L., Staelin, D.H., Strow, L.L., Susskind, J., 2003. AIRS/AMSU/HSB on the aqua mission: design, science objectives, data products, and processing systems. IEEE Trans. Geosci. Remote Sensing 41, 253–264.

Barkstrom, B.R., 1984. The earth radiation budget experiment (ERBE). Bull. Am. Meteorol. Soc. 65, 1170–1185.

Boyd, D.S., Curran, P.J., 1998. Using remote sensing to reduce uncertainties in the global carbon budget: the potential of radiation acquired in the middle infrared wavelengths. Remote Sensing Rev. 16, 293–327.

Curran, P.J., Atkinson, P.M., Foody, G.M., Milton, E.J., 2000. Linking remote sensing, land cover and disease. Adv. Parasitol. 47, 37–80.

Deeter, M.N., Francis, G.L., Edwards, D.P., Gille, J.C., McKernan, E., Drummond, J.R., 2002. Operational validation of the MOPITT instrument optical filters. J. Atmos. Oceanic Technol. 19, 1772.

Diner, D.J., Beckert, J.C., Bothwell, G.W., Rodriguez, J.I., 2002. Performance of the MISR instrument during its first 20 months in Earth orbit. IEEE Trans. Geosci. Remote Sensing 40, 1449–1466.

Diner, D.J., Beckert, J.C., Reilly, T.H., Bruegge, C.J., Conel, J.E., Kahn, R.A., Martonchik, J.V., Ackermann, T.P., Davies, R., Gerstl, S.A.W., Gordon, H.R., Muller, J.-P., Myneni, R.B., Sellers, P.J., Pinty, B., Verstraete, M.M., 1998. Multi-angle imaging spectroradiometer (MISR) instrument description and experiment overview. IEEE Trans. Geosci. Remote Sensing 36, 1072–1087.

Dister, S.W., Fish, D., Wood, B.L., 1997. Landscape characterization of peridomestic risk of Lyme disease using satellite imagery. Am. J. Trop. Med. Hyg. 57, 687–692.

Drummond, J.R., Mand, G.S., 1996. The measurements of pollution in the troposphere (MOPITT) instrument: overall performance and calibration requirements. J. Atmos. Oceanic Technol. 13, 314.

Dubayah, R., Wood, E.F., Lavallee, D., 1997. Multiscaling analysis in distributed modeling and remote sensing: and application using soil moisture. In: Quattrochi, D.A., Goodchild, M.F. (Eds.), Scale in Remote Sensing and GIS. CRC/Lewis Press, New York.

Fujisada, H., 1994. Overview of ASTER instrument on EOS AM-1 platform. Proc. SPIE 2268, 14–36.

Gillespie, A., Rokugawa, S., Matsunaga, T., Cothern, J.S., Hook, S., Kahle, A.B., 1998. A temperature and emissivity separation algorithm for advanced spaceborne thermal emission and reflection radiometer (ASTER) images. IEEE Trans. Geosci. Remote Sensing 36, 1113–1126.

Gleason, A.C.R., Prince, S.D., Goetz, S.J., Small, J., 2002. Effects of orbital drift on observations of land surface temperature measured by AVHRR thermal sensors. Remote Sensing Environ. 79, 147–165.

Goetz, S.J., Prince, S.D., Small, J., 2000. Advances in satellite remote sensing of environmental variables for epidemiological applications. Adv. Parasitol. 47, 289–307.

Gratz, N.G., 1999. Emerging and resurging vector-borne diseases. Ann. Rev. Entomol. 44, 51–75.

Green, R.M., Hay, S.I., 2002. The potential of Pathfinder AVHRR data for providing surrogate climatic variables across Africa and Europe for epidemiological applications. Remote Sensing Environ. 79, 166–175.

Greenwood, B., Mutabingwa, T., 2002. Malaria in 2002. Nature 415, 670–672.

Gutman, G.G., 1999. On the monitoring of land surface temperatures with the NOAA/AVHRR: removing the effect of satellite orbit drift. Intl. J. Remote Sensing 20, 3407–3413.

Hall, F.G., Huemmrich, K.F., Goetz, S.J., Sellers, P.J., Nickeson, J.E., 1992. Satellite remote sensing of surface energy balance: successes, failures and issues in FIFE. J. Geophys. Res. 97, 161–189.

Hansen, M.C., DeFries, R.S., Townshend, J.R., Sohlberg, R., Dimiceli, C., Carroll, M., 2002. Towards an operational MODIS continuous field of percent tree cover algorithm: examples using AVHRR and MODIS data. Remote Sensing Environ. 83, 303–319.

Hay, S.I., 1997. Remote sensing and disease control: past, present and future. Trans. R. Soc. Trop. Med. Hyg. 91, 105–106.

Hay, S.I., 2000. An overview of remote sensing and geodesy for epidemiology and public health application. Adv. Parasitol. 47, 1–35.

Hay, S.I., Lennon, J.J., 1999. Deriving meteorological variables across Africa for the study and control of vector-borne disease: a comparison of remote sensing and spatial interpolation of climate. Trop. Med. Intl. Health 4, 58–71.

Hay, S.I., Packer, M.J., Rogers, D.J., 1997. The impact of remote sensing on the study and control of invertebrate intermediate host and vectors for disease. Intl. J. Remote Sensing 18, 2899–2930.

Hay, S.I., Omumbo, J.A., Craig, M.H., Snow, R.W., 2000a. Earth observation, geographic information systems and plasmodium falciparum malaria in sub-Saharan Africa. Adv. Parasitol. 47, 173–215.

Hay, S.I., Randolph, S.E., Rogers, D.J. (Eds.), 2000. Remote sensing and geographic information systems in epidemiology, Advances in Parasitology. London, Academic Press.

Hay, S.I., Snow, R.W., Rogers, D.J., 1998. Predicting malaria seasons in Kenya using multitemporal meteorological satellite sensor data. Trans. R. Soc. Trop. Med. Hyg. 92, 12–20.

Heute, A., Didan, K., Miura, T., Rodriguez, E.P., Gao, X., Ferreira, L.G., 2002. Overview of the radiometric performance of the MODIS vegetation indices. Remote Sensing Environ. 83, 195–213.

Jin, M., Dickeson, R.E., 1999. Interpolation of surface radiative temperature measured from polar orbiting satellites to a diurnal cycle 1 without clouds. J. Geophys. Res. 104, 2105–2116.

Justice, C.O., Bailey, G.B., Maiden, M.E., Rasool, S.I., Strebel, D.E., Tarpley, J.D., 1995. Recent data and information system initiatives for remotely sensed measurements of the land surface. Remote Sensing Environ. 51, 235–244.

Justice, C.O., Townshend, J.R.G., Vermote, E.F., Masuoka, E., Wolfe, R.E., Saleous, N., Roy, D.P., Morisette, J.T., 2002. An overview of MODIS land data processing and product status. Remote Sensing Environ. 83, 3–15.

Justice, C.O., Vermote, E., Townshend, J.R.G., Defries, R., Roy, D.P., Hall, D.K., Salomonson, V.V., Privette, J.L., Riggs, G., Strahler, A., Lucht, W., Myneni, R.B., Knyazikhin, Y., Running, S.W., Nemani, R.R., Wan, Z., Huete, A.R., Van Leeuwen, W., Wolfe, R.E., Giglio, L., Muller, J.-P., Lewis, P., Barnsley, M.J., 1998. The moderate resolution imaging spectroradiometer (MODIS): land remote sensing for global change research. IEEE Trans. Geosci. Remote Sensing 36, 1228–1249.

Kahle, A., Palluconi, F., Hook, S., Realmuto, V.J., Bothwell, G., 1991. The advanced spaceborne thermal emission and reflectance radiometer (ASTER). Intl. J. Imaging Syst. Technol. 3, 144–156.

Kalluri, S.N.V., Dubayah, R.O., 1995. A comparison of atmospheric correction models for thermal bands of AVHRR over FIFE. J. Geophys. Res. 100, 25411–25418.

Kaufman, Y.J., Herring, D.D., Ranson, K.J., Collatz, G.J., 1998. Earth Observing System AM1 mission to Earth. IEEE Trans. Geosci. Remote Sensing 36, 1045–1055.

Kawanishi, T., Sezai, T., Ito, Y., Imaoka, K., Takeshima, T., Ishido, Y., Shibata, A., Miura, M., Inahata, H., Spencer, R.W., 2003. The advanced microwave scanning radiometer for the Earth Observing System (AMSR-E), NASDA's contribution to the EOS for global energy and water cycle studies. IEEE Trans. Geosci. Remote Sensing 41, 184–194.

Kazmi, S.J.H., Usery, E.L., 2000. Application of remote sensing and GIS for the monitoring of diseases: a unique research agenda for geographers. Remote Sensing Rev. 20, 45–70.

Lambrigtsen, B.H., Calheiros, R.V., 2003. The humidity sounder for Brazil – an international partnership. IEEE Trans. Geosci. Remote Sensing 41, 352–361.

Linthicum, K.J., Anyamba, A., Tucker, C.J., Kelly, P.W., Myers, M.F., Peters, C.J., 1999. Climate and satellite indicators to forecast Rift Valley Fever epidemics in Kenya. Science 285, 397–400.

NASA, 2003. Terra – the EOS flagship. http://terra.nasa.gov/.

Njoku, E.G., Jackson, T.J., Lakshmi, V., Chan, T.K., Nghiem, S.V., 2003. Soil moisture retrieval from AMSR-E. IEEE Trans. Geosci. Remote Sensing 41, 215–229.

NPOESS, 2003. National Polar-orbiting Operational Environmental Satellite System. http://www.ipo.noaa.gov/Technology/viirs_-summary.html.

Omumbo, J.A., Hay, S.I., Goetz, S.J., Snow, R.W., Rogers, D.J., 2002. Updating historical maps of malaria transmission duration in East Africa using remote sensing. Photogrammetric Eng. Remote Sensing 68, 161–166.

Parkinson, C.L., 2003. Aqua: an earth-observing satellite mission to examine water and other climate variables. IEEE Trans. Geosci. Remote Sensing 41, 173–183.

Parkinson, C.L., Chahine, M.T., Kummerow, C.D., Salomonson, V.V., 2003. Foreword to the EOS Aqua special issue. IEEE Trans. Geosci. Remote Sensing 41, 172.

Petitcolin, F., Vermote, E., 2002. Land surface reflectance, emissivity and temperature from MODIS middle and thermal infrared data. Remote Sensing Environ. 83, 112–134.

Price, J.C., 1984. Land surface temperature measurements from the split window channels of the NOAA 7 advanced very high resolution radiometer. J. Geophys. Res. 89, 7231–7237.

Randolph, S.E., 2000. Ticks and tick-borne disease systems in space and from space. Adv. Parasitol. 47, 217–243.

Randolph, S.E., 2001. Tick-borne encephalitis in Europe. Lancet 358, 1731–1732.

Rogers, D.J., Myers, M.F., Tucker, C.J., Smith, P.F., White, D.J., Brackenson, B., Eidson, M., Kramer, L.D., Bakker, B., Hay, S.I., 2002a. Predicting the distribution of West Nile Fever in North America using satellite sensor data. Photogrammetric Eng. Remote Sensing 68, 112–114.

Rogers, D.J., Randolph, S.E., Snow, R.W., Hay, S.I., 2002b. Satellite imagery in the study and forecast of malaria. Nature 415, 710–715.

Roy, D.P., Borak, J.S., Devadiga, S., Wolfe, R.E., Zheng, M., Descloitres, J., 2002. The MODIS land product quality assessment approach. Remote Sensing Environ. 83, 62–76.

Sachs, J., Malaney, P., 2002. The economic and social burden of malaria. Nature 415, 680–685.

Schmugge, T., French, A., Ritchie, J.C., Rango, A., Pelgrum, H., 2002. Temperature and emissivity separation from multispectral thermal infrared observations. Remote Sensing Environ. 79, 189–198.

Snow, R.W., Marsh, K., Le Sueur, D., 1996. The need for maps of transmission intensity to guide malaria control in Africa. Parasitol. Today 12, 455–457.

Snyder, W.C., Wan, Z., Zhang, Y., Feng, Y.-Z., 1998. Classification-based emissivity for land surface temperature measurement from space. Intl. J. Remote Sensing 19, 2753–2774.

Susskind, J., Barnet, C.D., Blaisdell, J.M., 2003. Retrieval of atmospheric and surface parameters from AIRS/AMSU/HSB data in the presence of clouds. IEEE Trans. Geosci. Remote Sensing 41, 390–409.

Tatem, A.J., Baylis, M., Mellor, P.S., Purse, B.V., Capela, R., Pena, I., Rogers, D.J., 2003. Prediction of bluetongue vector distribution in Europe and North Africa using satellite imagery. Vet. Microbiol. 97, 13–29.

Thomson, M.C., Connor, S.J., 2000. Environmental information systems for the control of arthropod vectors of disease. Med. Vet. Entomol. 14, 227–244.

Townshend, J.R.G., Justice, C.O., 2002. Towards operational monitoring of terrestrial systems by moderate-resolution remote sensing. Remote Sensing Environ. 83, 351–359.

USGS/NASA, 2002. Land Processes Distributed Active Archive Center. http://edcdaac.usgs.gov/gtopo30/gtopo30.html.

USGS/NASA, 2002. GTOPO30 DEM. http://edcdaac.usgs.gov/gtopo30/gtopo30.html.

Wan, Z., Li, Z.-L., 1997. A physics-based algorithm for retrieving land surface emissivity & temperature from EOS/MODIS data. IEEE Trans. Geosci. Remote Sensing 35, 980–996.

Warner, J.X., Gille, J.C., Edwards, D.P., Ziskin, D.C., Smith, M.W., Bailey, P.L., Rokke, L., 2001. Cloud detection and clearing for the Earth Observing System Terra satellite measurements of pollution in the troposphere (MOPITT) experiment. Appl. Opt. 40, 1269–1284.

Wielicki, B.A., Barkstrom, B.R., Baum, B.A., Charlock, T.P., Green, N., Kratz, D.P., Robert, R.B., Minnis, P., Smith, G.L., Wong, T., Young, D.F., Cess, R.D., Coakley, J.A., Crommelynck, D.A.H., Donner, L., Kandel, R., King, M.D., Miller, A.J., Ramanthan, V., Randall, D.A., Stowe, L.L., Welch, R.M., 1998. Clouds and Earth's Radient Energy System (CERES): algorithm overview. IEEE Trans. Geosci. Remote Sensing 36, 1127–1141.

Yamaguchi, Y., Fujisada, H., Tsu, H., Sato, I., Watanabe, H., Kato, M., Kudoh, M., Kahle, A.B., Pniel, M., 2001. ASTER early image evaluation. Adv. Space Res. 28, 69–76.

Yamaguchi, Y., Kahle, A.B., Tsu, H., Kawakami, T., Pniel, M., 1998. Overview of advanced spaceborne thermal emission and reflection radiometer (ASTER). IEEE Trans. Geosci. Remote Sensing 36, 1062–1071.